On Optimal Cooperative Conflict Resolution for Air Traffic Management Systems

Antonio Bicchi and Lucia Pallottino

Abstract—In this paper, we consider optimal resolution of air traffic (AT) conflicts. Aircraft are assumed to cruise within a given altitude layer and are modeled as a kinematic system with constant velocity and curvature bounds. Aircraft cannot get closer to each other than a predefined safety distance. For such system of multiple aircraft, we consider the problem of planning optimal paths among given waypoints. Necessary conditions for optimality of solutions are derived and used to devise a parameterization of possible trajectories that turns into efficient numerical solutions to the problem. Simulation results for a realistic aircraft conflict scenario are provided. A decentralized implementation of the optimal conflict resolution scheme is introduced that may allow free-flight coordination in a cooperative airspace management scheme. Impact of decentralization on performance and safety is finally discussed with the help of extensive simulations.

Index Terms—Air traffic (AT) management systems, conflict resolution, optimal control.

I. INTRODUCTION

AIRCRAFT coordination in increasingly crowded air space is becoming a major concern for air traffic control (ATC) authorities in the United States, Japan, and Europe [1], [2]. Conventional management schemes are being replaced by extensively computer-integrated air traffic management systems (ATMS) to maintain safety levels and increase throughput of congested airways. On the other hand, today's aircraft instrumentation and communications allow increasingly complex decisions to be taken on board, thus enabling a progressive move toward decentralized control scenarios often referred to as free-flight ATMS [3], [4].

Our work is aimed at providing efficient algorithms for conflict resolution and strategies, which are inherently safe and minimize fuel consumption, and to address pollution as well as economic concerns. In this paper, we apply optimal control and game theory (with particular reference to the branch addressing cooperative games, also known as team theory), to a kinematic model of AT.

Specifically, we will address the problem of planning motions of a system of multiple aircraft whose dynamics are described by the point-mass model [6], [7]. Aircraft conflicts are

modeled as collisions between the "conflict envelopes" that surround each aircraft. We make the central assumption that conflicts are to be solved while aircraft cruise within a fixed altitude layer. We also assume that aircraft dynamics and disturbances are dealt with, and "backstepped" to [8], first-order rate equations by autopilot controllers. Aircraft can thus be modeled in a purely kinematic fashion, as points in a plane with an associated fore axis and conflict envelope radius. The task of each vehicle is to reach a given goal configuration from a given start configuration (start and goal configurations represent way points planned for the aircraft by the higher level planner). Optimal solutions in the sense of minimizing total flight time will be considered.

Another important assumption we make is that all interacting aircraft cooperate toward optimization of a common goal as agents in the same team. This will apply to all aircraft in the centralized schemes to be discussed, while cooperation will only be assumed among aircraft that belong to the same cell of the information structure in our proposed decentralized scheme. Such a cooperative game approach has been considered already in the ATC literature (see, e.g., [9]) and should be contrasted with the antagonistic approach developed by [10], which results in single-aircraft strategies that are safe against worst-case maneuvers of all other potentially conflicting vehicles.

In the remaining sections of this paper, we will present the adopted model of AT (Section II) and discuss necessary conditions for optimality of conflict resolution schemes (Section III) from which numerical algorithms are derived (Section IV). Furthermore, the decentralized implementation of this AT management scheme will be described within the game—theoretic framework of teams (Section V). The performance and robustness of this decentralization scheme is assessed by means of simulation trials in Section VI.

II. MODELING

The point-mass aircraft model is a widely accepted description of dynamical effects encountered in civil aviation [11]. It consists of six equations, which, disregarding earth rotation and curvature, are

$$\dot{x} = V \cos\gamma \cos\chi \tag{1}$$

$$\dot{y} = V \cos\gamma \sin\chi \tag{2}$$

$$\dot{h} = V \sin\gamma \tag{3}$$

$$\dot{\gamma} = \frac{g}{V}(n\cos\varphi - \cos\gamma) \tag{4}$$

$$\dot{\chi} = \frac{g}{V}\frac{n\sin\varphi}{\cos\gamma} \tag{5}$$

$$\dot{V} = \frac{T-D}{m} - g\sin\gamma. \tag{6}$$

The authors are with the Department Electrical Systems and Automation and the Interdepartment Research Center "Enrico Piaggio," University of Pisa, 56100 Pisa, Italy (e-mail: bicchi@ing.unipi.it; lucia.pallottino@studenti.ing.unipi.it).

Fig. 1. Aircraft coordinate system.

Fig. 2. The airspace is structured in separate layers within which traffic conflicts have to be resolved.
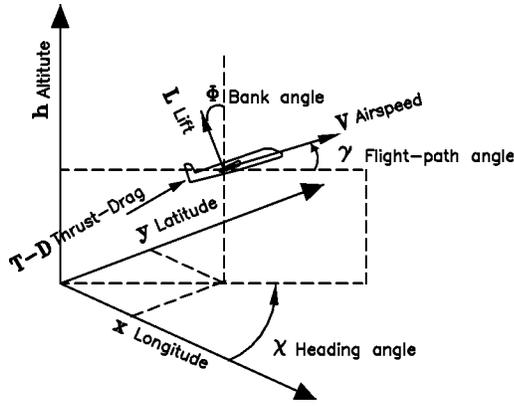
Here, x, y, h denote the components of the position of the center of gravity (CG) of the aircraft in a ground-based reference frame and are usually referred to as down range (or longitude), cross range (or latitude), and altitude, respectively. Angles are also defined with respect to the same frame: φ is the bank angle; χ is the heading angle; and γ is the flight-path angle (see Fig. 1). The ground-speed velocity V is assumed to be equal to airspeed, where T is the engine thrust, D is the aerodynamic drag, m the aircraft mass, g the gravity acceleration. Notice that the thrust depends on the altitude h, Mach number M, and throttle η by an assumedly known relationship $T = T(h, M, \eta)$. Also, it is assumed that the drag is a known function of h, M, and of the aerodynamic lift L ($D = D(h, M, L)$). The bank angle φ, the engine thrust T, and the load factor n are the control variables for the aircraft. The bank angle is commanded combining rudder and ailerons trims; the thrust is commanded by the engine throttle, and the load factor by elevators ($n = L/gm$). Using suitable nonlinear feedback of states (described in detail e.g., in [8] or [11]), the point-mass model can be linearized to Brunovsky's canonical form, i.e.,

$$\ddot{x} = U_x; \qquad \ddot{y} = U_y; \qquad \ddot{h} = U_h \qquad (7)$$

and the ensuing linear system can be easily controlled along planned trajectories $x_{\text{des}}(t)$, $y_{\text{des}}(t)$, $h_{\text{des}}(t)$ by adopting robust linear control techniques. The linearized equations (7), complemented with constraints on applicable inputs, form the basis of many aircraft trajectory optimization problems in the literature. Constraints are usually written in terms of original state variables and controls. The most common constraints considered are upper and lower bounds on airspeed, altitude, load factor, and thrust, and maximum climb and descent rates. These constraints can be translated in the linearized coordinates and controls, although this usually generates very involved formulations of the constraints that contribute a major obstacle toward analytic solution of optimization problems.

In AT conflict resolution, a crucial consideration is the separation constraint imposing that the so-called conflict envelopes of all aircraft do not overlap during flight. The current definition of conflict [12] of two aircraft involves that their altitude differs by less than 600 m (2000 ft) or that they get closer in a horizontal plane than 9260 m (5 nmi). The constraint can be visualized by considering for each aircraft a disk 600 m (2000 ft)
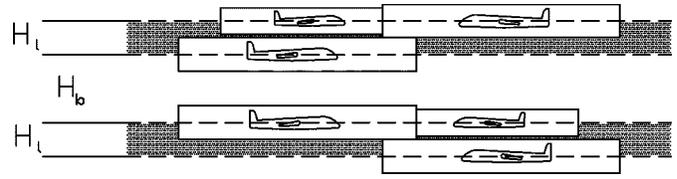
high and with a 4630 m (2.5 nmi) radius, centered in the aircraft representative point (e.g., the CG); in this case, the separation constraint imposes that the disks do not overlap during flight.

In order to make an analytical solution of the optimal AT conflict resolution problem possible and to gain the geometric insight that is often missing from numerically obtained solutions, the dynamic point-mass model is still too complex. Based on current practice in ATC, we introduce here a few simplifying assumptions that will make the problem tractable, while keeping the model reasonably close to real aircraft cruise conditions.

First, we consider ATC problems that possess an altitude-layered structure, in which the airspace is subdivided in horizontal layers of depth H_l (see Fig. 2). Each aircraft is supposed to be given waypoints belonging to the same layer and not to be allowed to leave the layer while cruising between the waypoints. Buffer layers of depth H_b are interposed between different altitude layers, where flight is forbidden. By imposing this structure on the airspace with $H_l \leq 600$ m $\leq H_b$, the conflict resolution problem is effectively decoupled, as no conflict can happen between aircraft of different layers. Conflicts need only to be resolved among aircraft flying within the same layer and only the distance between projections of the aircraft CGs on a horizontal plane need to be considered. As a consequence, to all practical purposes in the problem at hand, we may assume that longitudinal dynamics are regulated independently from the conflict resolution problem and disregard altitude variations in the model. A simplified planar aircraft model can then be adopted as

$$\dot{x} = u \cos \chi \qquad (8)$$
$$\dot{y} = u \sin \chi \qquad (9)$$
$$\dot{\chi} = \omega \qquad (10)$$

where $u \overset{\text{def}}{=} V \cos \gamma$ is the horizontal velocity, and $\omega \overset{\text{def}}{=} (L \sin \varphi / m)(1/u)$. Furthermore, we assume that forward dynamics (6) can be effectively controlled by the autopilot so as to track a given reference $\hat{V}(t) \cos \hat{\gamma}(t) = \hat{u}(t)$ with negligible errors, provided that the reference airspeed belongs to a given interval and is sufficiently smooth. Henceforth, we will regard u and ω as control inputs to the kinematic model (8) through (10). Bounds on the airspeed $V_{\min} \leq V \leq V_{\max}$ and on the flight-path angle $|\gamma| \leq \gamma_{\max}$ reflect in bounds on the new inputs as

$$V_{\min} \cos \gamma_{\max} \overset{\text{def}}{=} U_{\min} \leq u \leq U_{\max} \overset{\text{def}}{=} V_{\max}. \qquad (11)$$

The other input to the kinematic planar aircraft model is ω, whose physical dimensions are those of an angular velocity and will be termed *yaw rate*. Constraints on the yaw rate result from

constraints on the bank angle $|\varphi| \leq \varphi_{\max}$ and on the aerodynamic lift (proportional to the square of airspeed: $|L| \leq \beta_L V^2$). Accordingly, a bound on the yaw rate is obtained as

$$|\omega| \leq \frac{u}{R} \qquad (12)$$

where

$$R \stackrel{\text{def}}{=} \frac{V^2 \cos^2 \gamma_{\max}}{ng \sin |\varphi_{\max}|}.$$

The constant R has the dimensions of a length and, actually, in the kinematic model (8)–(10), (12) defines the minimum curvature radius that planar trajectories of the aircraft may achieve (the bound is actually achieved in planar cruise $\gamma = 0$).

A. Optimization Problem Statement

According to the previous discussion, consider N aircraft in the plane, whose individual configuration is described by $\xi_i = (x_i, y_i, \chi_i) \in \mathbb{R} \times \mathbb{R} \times S^1$. Each aircraft is assigned two waypoint configurations $\xi_{i,s}$ and $\xi_{i,g}$, respectively. The initial waypoint time is assigned and denoted by T_i^s. Assume aircraft are ordered such that $T_1^s \leq T_2^s \leq \ldots \leq T_N^s$. We denote by T_i^g the time at which the ith vehicle reaches its goal and let $T_i \stackrel{\text{def}}{=} T_i^g - T_i^s$. Motions of the ith airplane before T_i^s and after T_i^g are not of interest.

The ith aircraft motion is described by the control system $\dot{\xi}_i = f_i(\xi_i, u_i, \omega_i)$, with

$$f_i(\xi_i, u_i, \omega_i) = \begin{pmatrix} u_i \cos \chi_i \\ u_i \sin \chi_i \\ \omega_i \end{pmatrix}. \qquad (13)$$

All vehicles are subject to the following constraints.

1) Linear velocity is bounded: $U_{i,\min} \leq u_i \leq U_{i,\max}$.
2) Path curvature is bounded: $|\omega_i| \leq \Omega_i$, where $\Omega_i = (|u_i|/R_i)$ and $R_i > 0$ denotes the minimum curvature radius of trajectories for the ith vehicle.
3) Distance between two vehicles must remain larger than or equal to a given separation limit: $D_{ij}(t) = (x_j(t) - x_i(t))^2 + (y_j(t) - y_i(t))^2 - d_{ij}^2 \geq 0$, at all times t ($d_{ii} = 0$, $i = 1, \ldots, N$).

The length of the planar path joining the waypoints for the ith vehicle is

$$L_i = \int_{T_i^s}^{T_i^g} \sqrt{\dot{x}_i^2 + \dot{y}_i^2}\, dt = \int_{T_i^s}^{T_i^g} u_i\, dt. \qquad (14)$$

Consider the optimal conflict resolution problem for multiple vehicles defined as

$$\begin{cases} \min \sum_{i=1}^N J_i & \\ \dot{\xi}_i = f_i(\xi_i, u_i, \omega_i), & i = 1, \ldots, N \\ U_{i,\min} \leq u_i \leq U_{i,\max}, & i = 1, \ldots, N \\ |\omega_i| \leq \dfrac{|u_i|}{R_i}, & i = 1, \ldots, N \\ D_{ij}(t) \geq 0, & \forall t, i, j = 1, \ldots, N \\ \xi_i(T_i^s) = \xi_{i,s}, & \xi_i(T_i^g) = \xi_{i,g} \end{cases} \qquad (15)$$

where $J_i = L_i$ for shortest total path problems and $J_i = T_i$ for minimum total time problems. In this paper, we restrict to the case that the aircraft velocity u_i are constant. In this hypothesis, the two problems are equivalent and, henceforth, we will use the minimum total time formulation.

B. Formulation as an Optimal Control Problem

Notice that the cost for the total time problem $J = \sum_{i=1}^N T_i = \sum_{i=1}^N \int_{T_i^s}^{T_i^g} dt$ is not in the standard Bolza form. In order to use powerful results from optimal control theory, we rewrite the problem as follows. Let $h(t)$ denote the Heavyside function, i.e.,

$$h(t) = \begin{cases} 0, & t < 0 \\ 1, & t \geq 0 \end{cases}$$

and define the window function $w_i(t) = h(t - T_i^s) - h(t - T_i^g)$. Then the minimum total time cost is written as

$$J = \int_0^\infty \sum_{i=1}^N w_i(t)\, dt. \qquad (16)$$

Using the notation $\text{col}_{i=1}^N (v_i) = [v_1^T, \ldots, v_N^T]^T$, define the aggregated state $\xi = \text{col}_{i=1}^N(\xi_i)$, controls $u = \text{col}_{i=1}^N(u)$ and $\omega = \text{col}_{i=1}^N(\omega_i)$ and define the admissible control set Ω accordingly. Also, define the separation vector $D = [D_{12}, \ldots, D_{1N}, D_{23}, \ldots, D_{N-1,N}]$ and define the vector field $f(\xi, u, \omega) = \text{col}_{i=1}^N(f_i \omega_i)$. Finally, introduce matrices $\Gamma_i = \text{col}_{j=1}^N(\sigma_{ij}[1\ 1\ 1]^T)$, with $\sigma_{ij} = 1$ if $i = j$, else $\sigma_{ij} = 0$ and functions $\gamma_i(\xi(t), \bar{\xi}) = \Gamma_i(\xi(t) - \bar{\xi})$, where $\bar{\xi}$ is a vector of configurations. Our optimal control problem is then formulated as follows.

Problem 1: Minimize J subject to $\dot{\xi} = f(\xi, u, \omega)$, $\omega \in \Omega$, $D \geq 0$ and to the two sets of N interior-point constraints

$$\begin{aligned} \gamma_i(\xi(t), \xi_i^s) &= 0, & t &= T_i^s \\ \gamma_i(\xi(t), \xi_i^g) &= 0, & t &= T_i^g \text{(unspecified)}. \end{aligned}$$

III. NECESSARY CONDITIONS

Necessary conditions for problem 1 can be studied by adjoining the cost function with the constraints multiplied by unspecified LaGrange covectors. Omitting to write explicitly the extents of iterative operations when extending from 1 to N, let

$$\hat{J} = \sum_i \pi_i^s \gamma_i(\xi(T_i^s) - \xi_i^s) + \sum_i \pi_i^g \gamma_i(\xi(T_i^g) - \xi_i^g) + \int_0^\infty \sum_i w_i + \lambda^T \left(\dot{\xi} - f \right) + \nu^T D\, dt \qquad (17)$$

with λ and ν costates of suitable dimension and with $\nu_i = 0$ if $D_i > 0$, $\nu_i \geq 0$ if $D_i = 0$, and π_i^s and π_i^g are the unknown multiplier vectors corresponding to imposing initial and final conditions, respectively. Let the Hamiltonian be defined as

$$H = \sum_i w_i + \lambda^T f + \nu^T D. \qquad (18)$$

Substituting (18) in (17), integrating by parts, and computing the variation of the cost, one gets

$$\begin{aligned} \delta \hat{J} = &\sum_i \left[\lambda^T(T_i^{s-}) - \lambda^T(T_i^{s+}) + \pi_i^s \frac{\partial \gamma_i}{\partial \xi(T_i^s)} \right] d\xi(T_i^s) \\ &+ \sum_i \left[\lambda^T(T_i^{g-}) - \lambda^T(T_i^{g+}) + \pi_i^g \frac{\partial \gamma_i}{\partial \xi(T_i^g)} \right] d\xi(T_i^g) \\ &+ \sum_i \left[H(T_i^{g-}) - H(T_i^{g+}) + \pi_i^g \frac{\partial \gamma_i}{\partial T_i^g} \right] dT_i^g \\ &+ \int_0^\infty \left[\left(\dot{\lambda}^T + \frac{\partial H}{\partial \xi} \right) \delta \xi + \frac{\partial H}{\partial \omega} \delta \omega \right] dt \qquad (19) \end{aligned}$$

(recall that $dT_i^s \equiv 0$). Therefore, we have the following necessary conditions for an extremal solution:

$$\lambda_i(T_i^{s-}) = \lambda_i(T_i^{s+}) + \Gamma_i^T \pi_i^s \tag{20}$$

$$\lambda_i(T_i^{g-}) = \lambda_i(T_i^{g+}) + \Gamma_i^T \pi_i^g \tag{21}$$

$$H(T_i^{g-}) = H(T_i^{g+}) \tag{22}$$

$$\dot{\lambda}^T = -\frac{\partial H}{\partial \xi} \tag{23}$$

$$\frac{\partial H}{\partial \omega} \delta\omega = 0 \qquad \forall \delta\omega \text{ admiss.} \tag{24}$$

Extremal trajectories for the ith aircraft will be comprised in general of unconstrained arcs (with $D_{ij} > 0, \forall j \neq i$) and of constrained arcs, where the constraint is marginally satisfied ($\exists j: D_{ij} = 0$). We will accordingly distinguish the discussion of necessary conditions.

A. Extremal Unconstrained arcs

Suppose that for the ith vehicle, the separation constraints are not active in the interior of an interval $[t_i^a, t_i^b]$, $T_i^s \leq t_i^a < t_i^b \leq T_i^g$, i.e., $D_{ij}(t) > 0, j = 1, \ldots, N, t \in (t_i^a, t_i^b)$. The characterization of optimal solutions in the unconstrained case proceeds along the lines of the classical Dubins solution (see [13]–[15]). We succinctly report some results here for the reader's convenience.

Expanding (23), one gets

$$\left[\dot{\lambda}_{i1}, \dot{\lambda}_{i2}, \dot{\lambda}_{i3}\right] = [0, 0, \lambda_{i,1} u_i \sin\chi_i - \lambda_{i2} u_i \cos\chi_i]. \tag{25}$$

By integrating (25) one gets $\lambda_{i1}(t_i^a < t < t_i^b) = \overline{\lambda}_{i1}$, $\lambda_{i2}(t_i^a < t < t_i^b) = \overline{\lambda}_{i2}$, and $\lambda_{i3}(t_i^a < t < t_i^b) = \overline{\lambda}_{i1} y_i(t) - \overline{\lambda}_{i2} x_i(t) + \overline{\lambda}_{i3}$, with constant $\overline{\lambda}_{i,j}, j = 1, 2, 3$.

In light of these relationships, (20) and (21) imply that the costate components λ_{i1} and λ_{i2} are piecewise constant, with jumps possibly at the start and arrival time of the ith aircraft. The addend in the Hamiltonian relative to the ith vehicle and $\dot{\lambda}_{i3}$ can be written, respectively, as

$$H_i = 1 + u_i \rho_i \cos(\chi_i - \psi_i) + \lambda_{i3} \omega_i$$

and

$$\dot{\lambda}_{i3} = \rho_i u_i \sin(\chi_i - \psi_i) \tag{26}$$

where $\rho_i \overset{\text{def}}{=} \sqrt{\overline{\lambda}_{i1}^2 + \overline{\lambda}_{i2}^2}$ and $\psi_i \overset{\text{def}}{=} \text{a} \tan 2(\overline{\lambda}_{i2}, \overline{\lambda}_{i1})$.

As the model is not explicitly time-dependent, from Pontryagin minimum principle (PMP), we have $H_i(t) = \text{const.} \leq 0$ along time-extremal unconstrained arcs. Also, from PMP, we have that extremal arcs correspond to values of the control $-(u_i/R) \leq \omega_i \leq u_i/R$ that minimize the Hamiltonian.

Extremals of H_i within the open segment $\{|\omega| < u_i/R\}$ can only obtain if

$$\frac{\partial H_i}{\partial \omega_i} = \lambda_{i3} = \overline{\lambda}_{i1} y_i(t) - \overline{\lambda}_{i2} x_i(t) + \overline{\lambda}_{i3} = 0. \tag{27}$$

Notice that (27) is the equation of a straight line in the flight plane. In the following, such lines will be referred to as *supporting* lines.

If condition (27) holds on a time interval of nonzero measure, then $\dot{\lambda}_{i,3} = 0$ on the interval: this implies $\rho_i u_i \sin(\chi - \psi) = 0$, hence either $\rho_i = 0$ or $\chi = \psi \mod \pi$ and then $\omega_i = 0$.

In the former case ($\rho_i = 0$) we have $H_i = 1 + \lambda_{i3}\omega_i = \text{const.}$, hence, possible paths are either a line segment (denoted by a letter S) or an arc of circle (denoted by a letter C). Clearly, such solution applies only to initial and final waypoints lying on the same line or circle, respectively. For $\rho_i \neq 0$, conditions (27) and (26) imply $\chi_i = \psi_i \mod \pi$ and then $\omega_i = 0$ for $\rho_i \neq 0$. In such an interval, the aircraft is flying on a straight route (coinciding with a supporting line) in the horizontal x, y plane described in (27).

Other extremals of H_i occur at the boundaries of the input set $\omega = \pm u_i/R$. The sign of the minimizing yaw rate ω is opposite to that of λ_{i3}; in other words, the supporting line also represent the switching locus for the yaw rate input. Trajectories corresponding to $\omega_i = \pm u_i/R$ correspond to circles of minimum radius R followed counterclockwise or clockwise, respectively.

The following propositions can be proved to hold along extremal paths [15]:

1) the quantity $\lambda_{i3}(t) - \lambda_{i2}(t)y_i(t) + \lambda_{i1}(t)x_i(t)$ remains constant;
2) straight arcs and inflexion point (changes in curvature) belong to the supporting line;
3) any circular arc between two points where $\lambda_{i3} = 0$ has length $> \pi R$.

In the case of a single vehicle, the discussion of optimal unconstrained arcs can be further refined by several geometric arguments, for which the reader is referred directly to the literature [13]–[15]. Optimal paths for a single vehicle necessarily belong to either of two path types in the Dubins' sufficient family

$$\{C_a C_b C_e, C_u S_d C_v\} \tag{28}$$

where the subscripts, indicating the length of each piece, are restricted, respectively, to

$$b \in (\pi R, 2\pi R), \qquad a, e \in [0, b]$$
$$u, v \in [0, 2\pi R), \qquad d \geq 0. \tag{29}$$

A complete synthesis of optimal paths for a single Dubins vehicle is reported in [16]. The length of Dubins paths between two configurations denoted by $L_D(\xi_i^s, \xi_i^g)$ is then unique and defines a metric on $\mathbb{R}^2 \times S^1$. One simply has $L_D(\cdot, \cdot) = R(|a| + |b| + |c|)$ for a $C_a C_b C_e$ path, and $L_D(\cdot, \cdot) = R(|u| + |v|) + d$ for a $C_u S_d C_v$ path.

If a set of noncolliding Dubins' trajectories exists, then this is obviously a solution of the minimum total time problem. However, if with all combinations of possible independent Dubins trajectories a collision results, then the optimal solution must be searched among other longer extremal solutions or among paths with at least a constrained arc. While the latter case is discussed in the next subsection, we consider here an explicit characterization of all possible unconstrained extremal paths. This is done by distinguishing two cases as follows.

Case A—Unconstrained Extremal Paths Containing a Linear Segment: We know that all linear segments in an extremal path belong to a single supporting line. Furthermore linear segments have to be tangent to any circular arcs in the path. Hence, possible supporting lines are at most four [see Fig. 3(a)]. Switchings of ω_i among zero, u_i/R and $-u_i/R$ can only occur when the aircraft center is on the supporting line. As a consequence, for any extremal arc of type $C_u S_d C_v$ of length L, there exists a
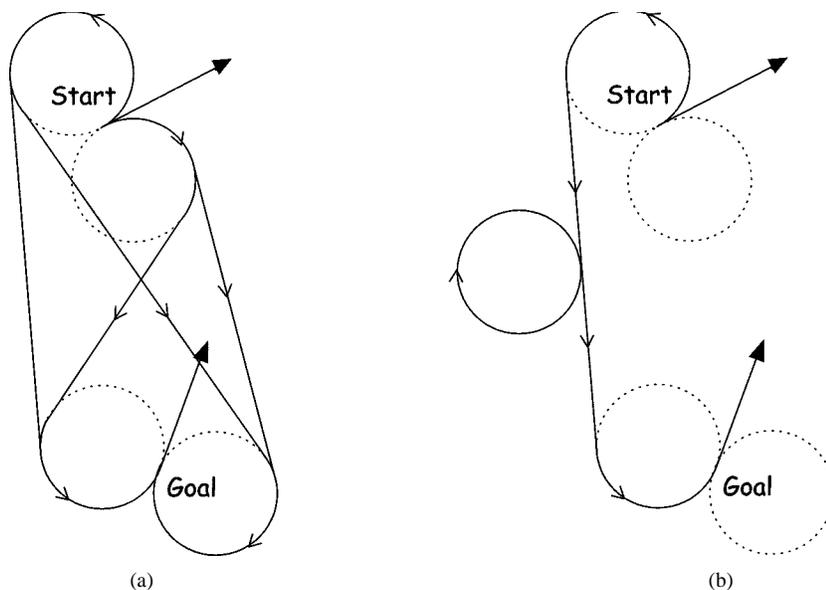
Fig. 3. (a) Four extremal arcs of type CSC joining two waypoints. (b) Extremal arc for the same waypoints including a "waiting" circle.

family of extremals of type $C_u S_{d_1} C_{2\pi} S_{d_2} \ldots S_{d_n} C_{2\pi} S_{d_{n+1}} C_v$, with $d = \sum_{i=1}^{n} d_i$, whose length is $L + 2n\pi$. Arcs of type $C_{2\pi}$ can be interpreted as "waiting" circular maneuvers for another aircraft to pass by and avoid collision [see Fig. 3(b)]. For any pair of waypoints, there are, therefore, four families of unconstrained extremal solutions of this type. For each family of extremals, the solution with smallest n for which there exist $d_1, d_2, \ldots, d_n$ that make it collision-free is the shortest possible solution within the family.

Case B—Unconstrained Extremal Paths Containing No Linear Segments: In this case, all inflexion points are aligned with a supporting line parallel to the lines joining the centers of tangent circles to the initial and final configurations (only the two pairs that can be followed with the same direction need be considered). Let D denote the distance between two centers: for any $n \geq \lceil D/4R \rceil$, $n \in \mathbb{N}$, one can have an extremal path formed by a concatenation of exactly $2n + 1$ circular arcs of type $C_{u_1} C_a C_b C_a \ldots C_a C_b C_a C_{u_2}$, where $a = -b$ and $|a| \geq \pi R$ (see Fig. 4). For any pair of waypoints, there are, therefore, two families of unconstrained extremal solutions of type $CCC \ldots CCC$, each containing a countable infinity of paths. The solution with smallest n, which is collision-free is the shortest possible solution within these families of extremals.

B. Extremal Constrained Arcs

Some further manipulation of the cost function is instrumental to deal with constrained arcs, i.e., arcs in which at least two vehicles are exactly at the critical separation ($D_{ij} = 0$, $i \neq j$). To fix some ideas, let us consider a constrained arc involving only vehicles 1 and 2. Along a constrained arc, the constraint and its derivatives must vanish, i.e.,

$$N = \begin{bmatrix} D_{12} \\ \dot{D}_{12} \end{bmatrix}$$
$$= \begin{bmatrix} (x_2 - x_1)^2 + (y_2 - y_1)^2 - d^2 \\ 2(x_2 - x_1)(\dot{x}_2 - \dot{x}_1) + 2(y_2 - y_1)(\dot{y}_2 - \dot{y}_1) \end{bmatrix} = 0 \tag{30}$$

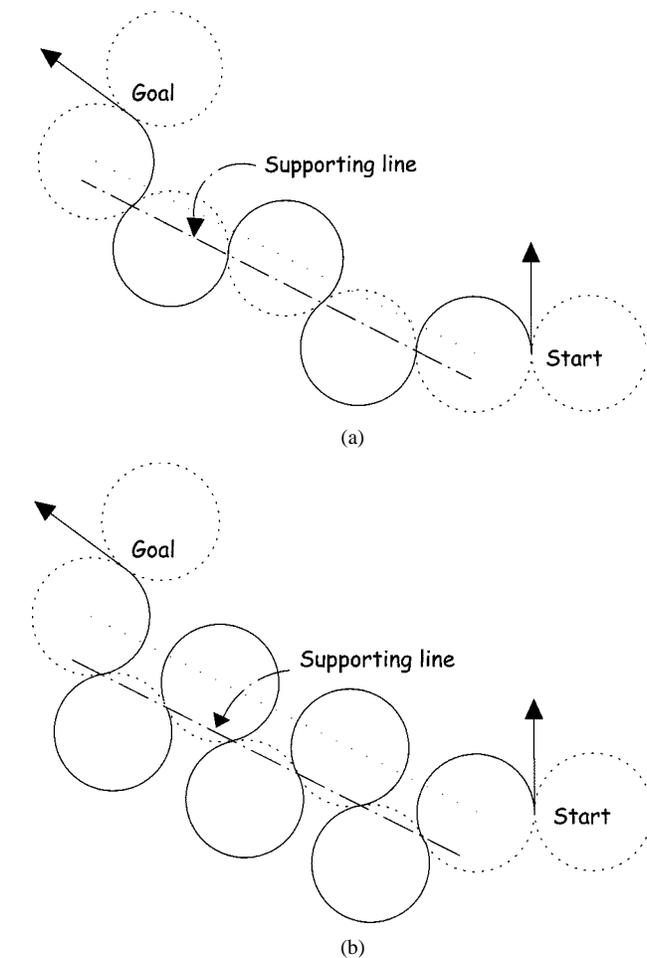
Fig. 4. Two unconstrained extremal solutions of type $CCC \ldots CCC$, with (a) $n = 2$ and (b) $n = 3$, respectively.

with $d = d_{12}$. Let ϕ be the direction of the segment joining the two vehicles so that

$$x_2 - x_1 = d \cos \phi,$$
$$y_2 - y_1 = d \sin \phi \tag{31}$$

a)   **b)**
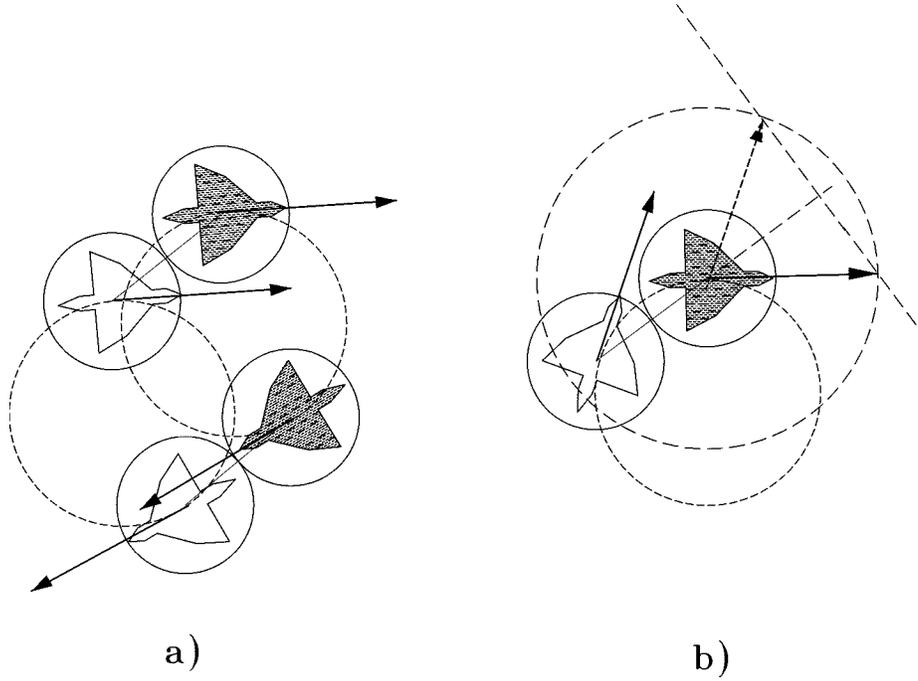
Fig. 5. Possible constrained arcs for two vehicles with the same airspeed: aircraft velocities may be (a) equal or (b) symmetric.

From the second equation in (30), one gets

$$
\begin{aligned}
(x_2 - x_1)(u_2 \cos \chi_2 - u_1 \cos \chi_1) \\
+ (y_2 - y_1)(u_2 \sin \chi_2 - u_1 \sin \chi_1) = 0
\end{aligned} \tag{32}
$$

and, using (31)

$$
u_1 \cos(\phi - \chi_1) - u_2 \cos(\phi - \chi_2) = 0. \tag{33}
$$

When the constraint is active, the two aircraft envelopes are in contact, and the relative orientation of the two vehicles must satisfy (33), which defines (for given u_1, u_2) two manifolds of solutions in the space $\{(\chi_1, \chi_2, \phi) \in S^1 \times S^1 \times S^1\}$ described as

$$
\textbf{a)} \quad \chi_2^a = \phi + \arccos\left(\frac{u_1}{u_2}\cos(\phi - \chi_1)\right) \tag{34}
$$

$$
\textbf{b)} \quad \chi_2^b = \phi - \arccos\left(\frac{u_1}{u_2}\cos(\phi - \chi_1)\right). \tag{35}
$$

The two solutions correspond to two different types ("a" and "b") of relative configurations in contact. For instance, for $u_1 = u_2$, one has

$$
\textbf{a)} \quad \chi_2^a = \chi_1 \tag{36}
$$
$$
\textbf{b)} \quad \chi_2^b = 2\phi - \chi_1. \tag{37}
$$

In case a), the two vehicles have the same velocity, while in case b), velocities are symmetric with respect to the segment joining the vehicles (see Fig. 5). In order to study constrained arcs of extremal solutions, it is useful to rewrite the cost function (17) as

$$
\overline{J} = \beta^T N + \sum_i \pi_i^s \gamma_i(\xi(T_i^s) - \xi_i^s) + \sum_i \pi_i^g \gamma_i(\xi(T_i^g) - \xi_i^g)
$$
$$
+ \int_0^\infty \sum_i w_i + \lambda^T\left(\dot{\xi} - f\right) + \mu \ddot{D}_{12}\, dt \tag{38}
$$

with $\mu \geq 0$ along a constrained arc. The jump conditions at the entry point of a constrained arc occurring at time τ are now

$$
\lambda_i(\tau^-) = \lambda_i(\tau^+) + \beta \left.\frac{\partial N}{\partial \xi}\right|_\tau \tag{39}
$$

$$
H(\tau^-) = H(\tau^+) \tag{40}
$$

where $H = \sum_i w_i + \lambda^T f + \nu^T \ddot{D}_{12}$, and

$$
\left(\frac{\partial N}{\partial \xi}\right)^T = 2 \begin{bmatrix}
(x_1 - x_2) & u_1 \cos \chi_1 - u_2 \cos \chi_2 \\
(y_1 - y_2) & u_1 \sin \chi_1 - u_2 \sin \chi_2 \\
0 & du_1 \sin(\phi - \chi_1) \\
(x_2 - x_1) & u_2 \cos \chi_2 - u_1 \cos \chi_1 \\
(y_2 - y_1) & u_2 \sin \chi_2 - u_1 \sin \chi_1 \\
0 & -du_2 \sin(\phi - \chi_2)
\end{bmatrix}.
$$

A further distinction among constrained arcs of zero and nonzero length should be done at this point. Consider first a *constrained arc of zero length* occurring at a generic contact configuration, which is completely described by the configuration of one aircraft (e.g., $\xi_c = \xi_1$), by the angle $\phi_c = \phi$ and by the contact type. Assume for the moment that there is only one constrained arc of zero length in the optimal path between start and goal of the two aircraft. Equation (39), taking into account that costates of each aircraft are determined (once the start, goal, and contact configurations are fixed) up to constants $\rho_i(\tau^-)$, $\rho_i(\tau^+)$ in (26), provides a system of six equations in six unknowns of the form

$$
A(\xi_c, \phi_c) \begin{bmatrix}
\rho_1(\tau^-) \\
\rho_1(\tau^+) \\
\rho_2(\tau^-) \\
\rho_2(\tau^+) \\
\beta_1 \\
\beta_2
\end{bmatrix} = 0
$$

where the explicit expression of matrix $A(\xi_c, \phi_c)$ for each contact type can be easily evaluated in terms of $\xi_1^s, \xi_1^g, \xi_2^s, \xi_2^g$, and is omitted here for space limitations. Nontriviality of costates implies that (ξ_c, ϕ_c) must satisfy $\det(A) = 0$. A further constraint on contact configurations is implied by the equality of flight times from start to contact for the airplanes, which is expressed in terms of Dubins distances as $L_D(\xi_1^s, \xi_c)/u_1 = L_D(\xi_2^s, \xi_c')/u_2$, where ξ_c' denotes the configuration of aircraft 2 at contact that is uniquely determined for each contact type. If m constrained arcs of zero length are present in an optimal solution, similar conditions apply (with start and goal configurations suitably replaced by previous or successive contact configurations), yielding $2m$ equations in $4m$ unknowns. On the other hand, *constrained arcs of nonzero length* can be studied by recasting the problem in a reduced configuration space. Solutions consist in optimal trajectories for aircraft that remain constantly at the minimum tolerated distance. As such, these solutions are of interest in coordinating flight of aircraft formations (employed, e.g., for reducing fuel consumption by reducing aerodynamic drag) and have been studied in detail by the authors in [17]. However, this type of borderline solution seem to be unacceptable in conflict resolution for commercial AT. Henceforth, we disregard the possibility that in an optimal resolution of a conflict, there are constrained arcs of nonzero length.

IV. NUMERICAL COMPUTATION OF SOLUTIONS

The necessary conditions studied in the previous sections provide useful hints in the search for an optimal solution to the problem of planning trajectories of N aircraft in a common airspace. Although a complete synthesis has not been obtained so far, we will describe in this section an algorithm that finds suboptimal solutions to the optimal planning problem under some simplifying assumptions.

Based on the discussion of the sections above, the optimal conflict resolution paths for multiple aircraft may include multiple waiting circles (Fig. 3) or winding paths (Fig. 4) and constrained arcs of both zero and nonzero length. However, based on heuristic considerations about acceptability to passengers, we assume, henceforth, that the following are not allowed:

h1 constrained arcs of nonzero length (see Section V);
h2 multiple zero-length constrained arcs among the same aircraft;
h3 concatenations of arcs of type $CC\ldots C$ (see Section III-A).

Moreover, for simplicity of description, in the following we assume that all aircraft have equal geometric characteristics and equal speed (removal of these hypotheses does not alter substantially the algorithm described below).

Consider first the case of two aircraft. If the Dubins' trajectories joining the way-points configurations do not collide, then this is the optimal solution. Otherwise we compute the shortest contact-free solution with waiting circles and let its length be L_f. Hence, we look for a solution with a concatenation of two Dubins' paths and a single constrained zero-length arc of either type a) or b) for both aircraft. Such solution can be searched over a two-dimensional submanifold of the contact configuration space ($\mathbb{R}^2 \times S^1 \times S^1$). The optimal solution can be obtained by using any of several available numerical constrained optimization routines: computation is sped up considerably by using very efficient algorithms made available for evaluating Dubins' paths [16]. The length L_c of such solution is compared with L_f, and the shorter solution is retained as the two-aircraft optimal conflict management path with at most a single constrained zero-length arc (OCMP21, for short). Some examples of OCMP21 solutions are reported in Fig. 6, where two aircraft are involved in a conflict and the solution is a concatenation of two Dubins paths, before and after the contact, respectively. This example, as well as others to be presented, refer to a scenario with two equal aircraft, with mass $m = 83\,250$ kg (185 klbm), airspeed $V_{\max} = 150$ m/sec (500 ft/sec), load factor $n = 1.12$, max. bank angle $\varphi_{\max} = 27°$, hence, (for $\gamma = 0$), the minimum curvature radius results $R = 4445$ m (2.4 nmi) [11].

If N aircraft fly in a shared airspace, their possible conflicts can be managed with the following multilevel policy.

Level 0 Consider the unconstrained Dubins paths of all aircraft, which may be regarded as N single-aircraft optimal-conflict management paths, or OCMP10. If no collision occurs, the global optimum is achieved and the algorithm stops. Otherwise, compute the shortest contact-free paths (with waiting circles) and go to next level.

Level 1 Consider the $M = 2\binom{N}{2}$ possible solutions with a single contact [of either type a) or b)] between two aircraft and possibly waiting circles for other aircraft and compute the shortest path in this class. If this is longer than the shortest path obtained at Level 0, exit. Otherwise, continue.

Level $m \geq 2$ Consider the $M \prod_{\ell=1}^{m-1} (M - 2^\ell)$ possible solutions involving m zero-length constrained arcs between different pairs of aircraft and (possibly) waiting circles for other aircraft and compute the shortest path in this class. If this is longer than the shortest path obtained at level $m - 1$, exit. Otherwise, continue.

A few three-aircraft conflict resolution trajectories at different levels are reported in Fig. 7.

When the number of aircraft increases, the number of optimization problems to be solved grows combinatorially. However, in practice, it is hardly to be expected that conflicts between more than a few aircraft at a time have to be managed that require solutions of a level higher than 2.

V. DECENTRALIZED IMPLEMENTATION FOR FREE FLIGHT

In decentralized ATMS schemes, each agent (aircraft) is allowed to take decisions autonomously based on the information that is available at each time. Several models of decentralized ATC are conceivable, which may differ in the degree of cooperative/competitive behavior of the agents and in the information structure [11], [10]. In this paper, we consider a cooperative scheme, which falls within the scope of the theory of teams (cf. [18], [19]). In particular, we consider a scheme in which
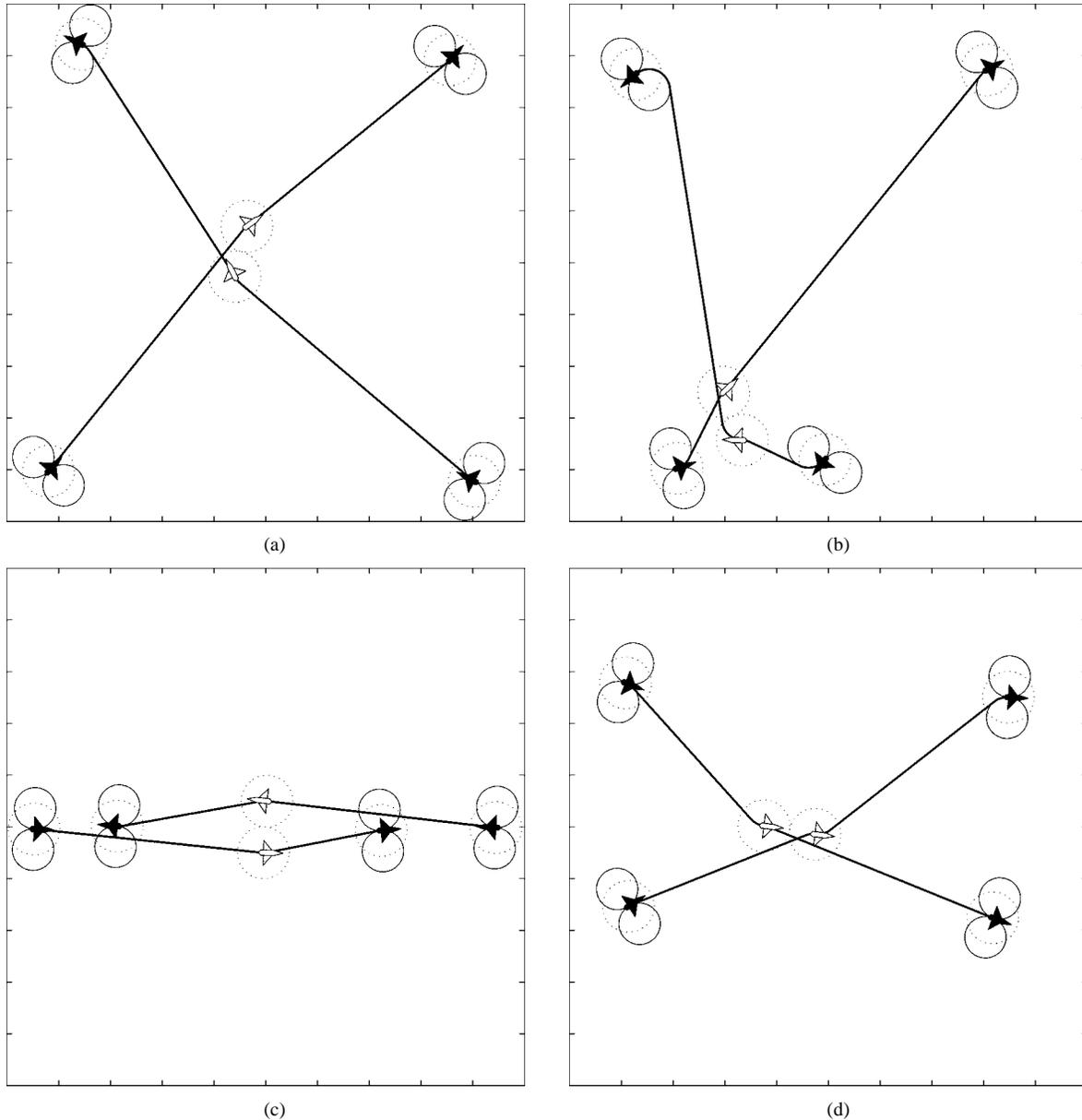
Fig. 6.   Numerically computed solutions to optimal cooperative conflict resolution for two aircraft. Minimum curvature circles are reported at the start and goal configurations, along with safety discs of radius $d/2$ (dashed).

- the ith agent has information on the state and goals of all other agents, which are at a distance less than an "alert" radius A_i;
- each agent plans its flight according to an optimal strategy, which consists of minimizing the sum of the time-to-goals of all aircraft of which the agent is aware.

Let $S_i(\tau)$ denote the set of indexes of aircraft within distance A_i from the ith aircraft at time τ. The goal of the ith agent at time τ with information S_i is, therefore, to minimize

$$\mathbf{J}_{i,S_i}(\tau) = \sum_{j \in S_i} \int_{\tau}^{T_j} dt \qquad (41)$$

under the constraints $D_{ij}(\xi_i, \xi_j) \geq 0, \forall j \in S_i$. Obviously, when all A_i are large with regard to the dimension of the considered airspace, each agent solves the same problem the centralized controller would solve and the resulting performance would be equal (although with N-fold computational redundancy).

When, during execution of flight maneuvers that were planned based on a certain information structure $I = (S_1, \ldots, S_N)$, an aircraft i with $i \notin S_j$ gets at distance A_j from aircraft j, the information structure is updated, and optimal paths are replanned according to the new cost and constraints for aircraft j.

The system resulting from the above decentralized ATMS scheme is described by a set of continuous variables ξ_i, ω_i, $i = 1, \ldots, N$, and a set of variables S_i that take values over discrete sets. To each different information structure I_k there corresponds a working mode for the system, i.e., dynamics (13) driven by controls optimizing J_{i,S_i} under constraints $D_{ij} > 0$, $j \in S_i$, which can be computed as described in previous sections of this paper. The resulting hybrid system is composed of a finite-state machine and of associated continuous-time dynamic systems, transitions among states being triggered by conditions on the continuous variables.
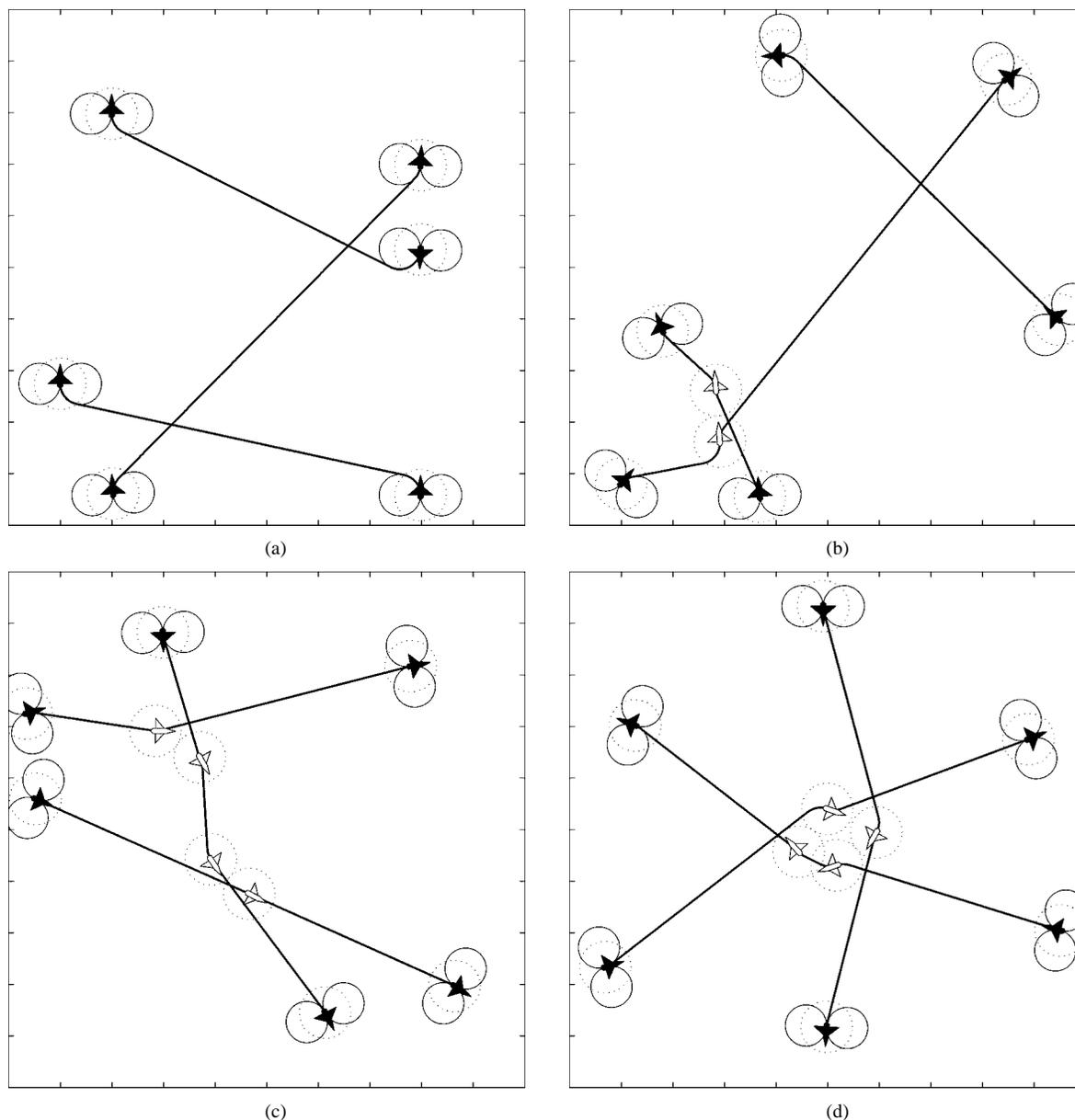
Fig. 7. Four cases of three-aircraft conflict resolution. (a) Conflict is resolved at level 0. (b) Level 1 solution. (c) Level 2 solution. (d) Level 2 resolution that generates a roundabout-like maneuver.

For instance, in the case with $N = 3$, $A_1 = A_2 = A_3$, there are eight possible states (modes of operation), corresponding to different information structures I_k (see Fig. 8).

At every state transition, each agent evaluates in real-time the optimal steering control from the current position to the goal for itself as well as for all other aircraft within its alert radius. Only the control policy evaluated by an agent for itself is then executed, as the one calculated for others may ignore part of the information available to them (as e.g., it happens in states I_5, I_6, and I_7 in Fig. 8).

All optimal policies coincide for large A_is. However, for small alert radii, the localization of conflict solution might give raise to a cascading effect on other conflicts, with possibly destabilizing consequences. To avoid this problem, a possible solution is to make the information structure *reflexive* and *transitive*. In our setup, an information structure is reflexive if $i \in S_j \Rightarrow j \in S_i$; it is transitive if $i \in S_j$ and $j \in S_k$

$\Rightarrow i \in S_k$. Imposing a reflexive and transitive structure however might quickly destroy advantages of decentralization by increasing the size of the optimization problems to be solved. In the following, we will not impose such conditions, and will leave the provision of safety guarantees as a fundamentally open problem for the hybrid model in Fig. 8.

The decentralized solutions of a two-agent conflict management problem is reported in Fig. 9. It can be observed that the two aircraft initially are not aware of each other and follow their unconstrained Dubins path, which would be bound for collision (indicated by little crosses). When they enter the alert zones (this happens roughly at the third step after start in Fig. 9), an OCMP21 is obtained by both agents. Notice that, in this two-agent problem with equal alert radius, the same problem is solved by both agents by means of the same algorithm, hence, the same solution is obtained. Aircraft start following their modified paths, which differ from both the unconstrained Dubins
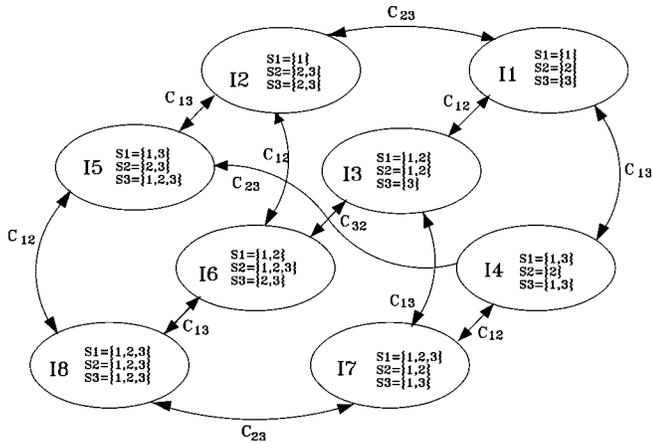
Fig. 8. A decentralized ATMS with three aircraft having equal alert radius. Each node in the graph corresponds to different costs and constraints in the agents' optimal steering problem. Optimizing controllers for such problems cause different continuous time dynamics at each node. Switching between modes is triggered when an airplane enters or exits the alert neighborhood of another ($D_{i,j}$ changes sign).
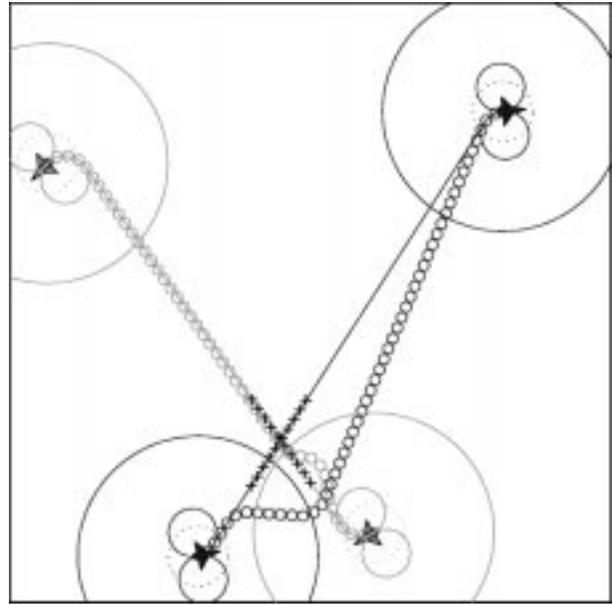

Fig. 9. Decentralized solution of the two-agent conflict management problem (trajectories traced by small circles). Alert discs are drawn in solid lines around the initial and final configurations of agents. The unconstrained Dubins' paths are superimposed for reference.
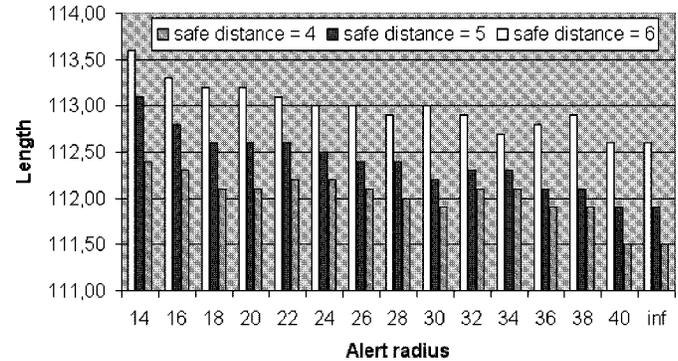

Fig. 10. Total length flown by aircraft at varying the alert zone radius. The measures are in nautical miles.

paths and the optimal paths that would have been computed by a centralized planner.

VI. PERFORMANCE AND FAULT TOLERANCE OF THE DECENTRALIZED IMPLEMENTATION

A number of issues should be considered when deciding on the appropriate level of centralization such as efficiency, complexity, robustness, and flexibility.

In order to assess the effects of increasing decentralization in ATMS, we performed a number of simulations whose results are reported below.

In particular, we experimentally compared results obtained by a centralized planner with those achieved by several decentralized planners with decreasing alert zone radius. The alert zone radius can be regarded as an inverse measure of the degree of centralization for an information structure such as that introduced in the section above.

The first set of simulations concerns performance evaluation. The performance measure, i.e., the total length cumulatively flown by all airplanes for the problem described in Fig. 9 has been calculated for three different values of the safety radius. Results of simulations are reported in Fig. 10 and show that the increase of the alert zone radius entails a rather smooth decrease of the total length flown by aircraft. As an effect of the presence of local minima in the numerical optimization process, the length does not decrease monotonically as it would have been expected.

The second set of simulations was performed to assess fault tolerance and involved the same scenario and planning algorithms under degraded control conditions. In particular, we assume that some of the controllers fail during flight. The jth failure period (or "crisis") of the ith controller is initiated at time $t_{i,j}$ (with $T_i^s < t_{i,j} < T_i^g$) and resolved at time $t_{i,j} + \Delta_{i,j}$. During a crisis, the ith controller provides random erroneous references for the ith aircraft. At the end of a crisis, the controller is supposed to access correct data again and to replan accordingly. Under decentralized ATC, other agents are able to maintain their correct operation mode and replan in real time to try and avoid collisions.

It is important to notice that two crisis scenarios are possible, corresponding to whether or not the crisis of the ith controller is detected by other agents operating regularly. We assume that whenever a critical situation is detected by any agent, then the operating mode of the agent is switched from the cooperative strategy described in this paper to an antagonistic approach such as that reported in [10]. Therefore, we assume in what follows that failures of one agent are not detected by other agents.

In simulations reported below, the crisis periods have been chosen to have constant length $\Delta_{i,j} = \Delta, \forall i, j$ in all simulation runs: Δ is set to approximately 3% of the expected flight time between the waypoints. The initial crisis time $t_{i,j}$ is a uniformly distributed random variable over both the aircraft index and the flight time span. Casual references for critical aircraft are generated by applying the usual planning algorithm to a random goal configuration.
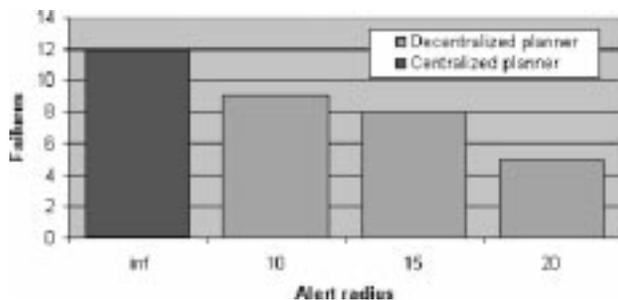
Fig. 11. Fault tolerance to controller failures at varying the degree of decentralization. The number of accidents is relative to 100 crisis situations. Labels on the x axis refer to alert radii measured in nautical miles.

As a figure of fault tolerance of ATMS schemes, we consider the number of accidents for 100 crisis situations. Results of simulations, relative to the same initial scenario as in Fig. 9, are reported in Fig. 11. In the centralized ATMS case, all aircraft are assumed to receive random flight directions from the single centralized controller when this enters a critical situation: 12 crises out of 100 led to accidents in this configuration. The percentage of unrecoverable crises under a decentralized strategy is reduced to roughly 9% with an alert radius of 10 nmi down to 5% when the radius is doubled. These results agree with the expectation that introducing decentralization can achieve some degree of robustness of ATC with respect to centralized schemes. The fact that robustness is enhanced by increasing the alert radius is clearly explained by the degree of computational redundancy introduced.

VII. CONCLUSION

In this paper, we have studied the problem of planning optimal conflict resolution maneuvers for kinematic models of aircraft flying in a horizontal plane with constant velocity. Necessary conditions have been derived and an algorithm for numerically finding suboptimal solutions has been described. A decentralized implementation has been introduced, and extensive simulations have been employed to establish its performance and fault tolerance.

Future work on this topic will address the problem of finding a complete optimal synthesis at least for the simplest cases ($N = 2$), and extending to the case of variable longitudinal velocity. Further refinement of the algorithm can be sought, to exploit more of the rich structure of optimal solutions. The case when the aircraft speed can be varied needs also to be studied in detail. An ever standing issue is that of computational efficiency of the optimization algorithm, to achieve real-time solutions for conflicts involving more than three aircraft. A crucial problem is to analyze in depth the properties of the hybrid system in Fig. 8, and to determine exact regions of state–space for which safety guarantees can be given for given perturbation levels.

ACKNOWLEDGMENT

REFERENCES

[1] Honeywell Inc., "Markets Rep.,", Tech. Rep. NASA Contract AATT, 1996.
[2] T. S. Perry, "In search of the future of air traffic control," *IEEE Spectrum*, vol. 34, pp. 18–35, Aug. 1997.
[3] RTCA Task Force 3, "Final Tech. Rep.: Free flight implementation,", Washington, DC, Radio Tech. Commission Aeronaut., Oct. 1995.
[4] Ed. Board, "Special report on free flight," *Aviation Week Space Technol.*, vol. 143, pp. 38–48, July 1995.
[5] C. Tomlin, G. Pappas, J. Kosecka, J. Lygeros, and S. Sastry, "Advanced air traffic automation: Acase study in distributed decentralized control," in *Control Problems in Robotics and Automation*, B. Siciliano and K. Valavanis, Eds. New York: Springer-Verlag, 1997, pp. 261–295.
[6] R. C. Nelson, *Flight Stability and Automatic Control*. New York: McGraw-Hill, 1989.
[7] B. Etkin, *Dynamics of Atmospheric Flight*. New York: Wiley, 1982.
[8] G. Meyer, R. Su, and L. R. Hunt, "Application of nonlinear transformations to automatic flight control," *Automatica*, vol. 20, pp. 103–107, 1984.
[9] Y.-J. Chiang, J. T. Klosowski, C. Lee, and J. S. B. Mitchell, "Geometric algorithms for conflict detection/resolution in air traffic management," in *Proc. 36th IEEE Conf. Decision and Contr.*, San Diego, CA, 1997, pp. 1835–1840.
[10] C. Tomlin, G. J. Pappas, and S. Sastry, "Conflict resolution for air traffic management: A case study in multi-agent hybrid systems," *IEEE Trans. Automat. Contr.*, vol. 43, pp. 509–521, Apr. 1998.
[11] P. K. Menon, G. D. Sweriduk, and B. Sridhar, "Optimal strategies for free-flight air traffic conflict resolution," *J. Guidance, Contr., Dynam.*, vol. 22, no. 2, pp. 202–211, Mar.–Apr. 1999.
[12] H. Erzberger and W. Nedell, "Design of automated system for management of arrival traffic," NASA Ames Res. Ctr. Tech. Memo 102 201, June 1989.
[13] L. E. Dubins, "On curves of minimal length with a constraint on average curvature and with prescribed initial and terminal positions and tangent," *Amer. J. Mathematics*, vol. 79, pp. 497–516, 1957.
[14] H. J. Sussmann and G. Tang, "Shortest paths for the Reeds–Shepp car: A worked out example of the use of geometric techniques in nonlinear optimal control," SYCON, Rutgers Ctr. Syst. Contr. Tech. Rep. 91-10, New Brunswick, NJ, Tech. Rep. 91–10, Sept. 1991.
[15] J. D. Boissonnat, A. Cerezo, and J. Leblond, "Shortest paths of bounded curvature in the plane," in *Proc. Int. Conf. Robot. Automation*, Nice, France, May 1992, pp. 2315–2320.
[16] X. N. Bui, P. Souères, J.-D. Boissonnat, and J.-P. Laumond, "Shortest path synthesis for Dubins nonholonomic robots," in *Proc. Int. Conf. on Robotics and Automation*, San Diego, CA, Apr. 1994, pp. 2–7.
[17] A. Bicchi and L. Pallottino, "Optimal planning for coordinated vehicles with bounded curvature,," in Proc. Int. Workshop Algorithmic Foundations Robot., B. Donald, K. Lynch, and D. Rus, Eds. Dartmouth, NH, Mar. 2000, to be published.
[18] Y. C. Ho and K. C. Chiu, "Team decision theory and information structures in optimal control problems—Part I," *IEEE Trans. Automat. Contr.*, vol. AC-17, pp. 15–21, 1972.
[19] M. Aicardi, F. Davoli, and R. Minciardi, "Decentralized optimal control of markov chains with a common past information set," *IEEE Trans. Automat. Contr.*, vol. AC-32, pp. 1028–1031, Nov. 1987.

Antonio Bicchi was born in Toscana, Italia, in 1959. He received the Laurea degree from the University of Pisa, Italy, in 1984, and the Ph.D. degree from the University of Bologna, Italy, in 1988.

He has been a Postdoctoral Scholar at the Massachusetts Institute of Technology (MIT) Artificial Intelligence Laboratory, Cambridge, from 1988 to 1990. He is currently an Associate Professor of systems theory and robotics in the Department of Electrical Systems and Automation (DSEA), University of Pisa. Since 1990, he has been leading the Robotics Group at the Interdepartmental Research Center "E. Piaggio," University of Pisa. His main research interests within robotics are in dextrous manipulation, including force/torque and tactile sensing, haptics and sensory control, dynamics, kinematics, and control of complex mechanichal systems, and motion planning and control for nonholonomic and quantized systems.

Lucia Pallottino was born in Rome, Italy, in 1974. She received the Laurea degree in mathematics from the University of Pisa, Italy, in 1997. She is currently working toward the Ph.D. degree in robotics and industrial automation from the Department of Electrical Systems and Automation (DSEA), University of Pisa. Her main research interests within robotics are in motion planning and control for nonholonomic systems and air traffic management.